

# CORRELATING THE DISORDER-TO-ORDER TRANSITION OF BIPHENYL AND NAPHTHALENE ON $\text{Al}_2\text{O}_3$ TO NUCLEATION-CRYSTALLIZATION KINETICS

Alan O. Lopez\*, Maxwell K. Fuller\*, Caleb D. Tobey\*, Brandon X. Moses\* and A.M. Nishimura†

Department of Chemistry, Westmont College, Santa Barbara, CA 93108

## Abstract

The disorder-to-order transition in vapor deposited biphenyl and naphthalene were correlated to nucleation-crystallization kinetics. A curve fitting program was used to extract the parameters that describe both the rate and dimensionality of the process. In addition, the effects an impurity such as methanol that percolates the chromophoric adlayer has on the nucleation-crystallization kinetics was investigated. The results were that both biphenyl and naphthalene's dimensionality of the process was about half. However, the rates with the impurity was 20% slower for biphenyl, but for naphthalene, the rate was an order of magnitude faster with the impurity.

†Corresponding author: nishimu@westmont.edu

\*Undergraduate researchers and co-authors

Keywords: biphenyl, naphthalene, methanol, disorder-to-order transition, nucleation-crystallization kinetics, Avrami kinetics

Submitted: November 28, 2025 Accepted: December 2, 2025 Revision received: December 3, 2025 Published: December 4, 2025

## Introduction

For many years, the disorder-to-order transition in both biphenyl and naphthalene that had been vapor deposited on  $\text{Al}_2\text{O}_3$  have been routinely observed.<sup>1-4</sup> These studies involved not only the neat adsorbates, but also the molecular interactions that occur with other molecules as an underlayer.<sup>1-4</sup> Recently, these disorder-to-order transitions in biphenyl and naphthalene were postulated to be correlated to nucleation-crystallization kinetics.<sup>5-7</sup> In this study, a more focused attempt has been made to determine if nucleation-crystallization kinetics models fit the disorder-to-order transitions in these two systems. In addition, the effect of an impurity, methanol, was used to observe the change in the kinetics of nucleation-crystallization.

## Experimental

Biphenyl, naphthalene, were of the highest purity (> 99%) that could be purchased from commercial sources (Sigma-Aldrich, St. Louis, MO). The details of the experimental set-up were described in detail in the previous papers<sup>1-7</sup> and are summarized here. These compounds were placed in a sample holder attached to one end of a precision leak valve for vapor deposition that led into the main ultra-high vacuum chamber. The substrate was a single crystal of  $\text{Al}_2\text{O}_3$  (0001) that was suspended on the lower end of a liquid nitrogen cryostat.

The fluorophores were optically pumped with a high pressure mercury lamp. A 0.25 m monochromator was used to select a 250 nm wavelength. Resistive heating of the  $\text{Al}_2\text{O}_3$  was done by sending current through a thin tantalum foil that was in thermal contact with the substrate. A process controlling code was written in LabVIEW that monitored the surface temperature via a thermocouple attached to the  $\text{Al}_2\text{O}_3$ . A feedback program controlled the current which allowed the temperature ramp for the experiment to be linear with a certainty of  $1.98 \pm 0.01 \text{ K s}^{-1}$ . This level of linearity allows temperature to be equated to time, as will be noted later. During the temperature programmed desorption, TPD, the program also took the fluorescence spectra every 300 ms using a spectrometer with input connected to a fiber-optic cable that fed into the chamber. A lens was mounted on the end to collect the fluorescence. The spectra were processed via a MatLab code and used to create the wavelength-resolved TPD figures shown below.

To ensure a clean surface after each experiment, the  $\text{Al}_2\text{O}_3$  was heated to 300 K. Temperature ramps to higher temperatures did not indicate any other adsorbates.<sup>1-7</sup>

The activation energy for desorption,  $E_a$ , was calculated by Redhead analysis using the mass spectral peak desorption temperature,  $T_p$ .<sup>8-10</sup> As described by King, first-order desorption kinetics was assumed.<sup>8-10</sup> The uncertainties in the desorption temperatures lead to a propagated error in the activation energies of  $\pm 2\%$ , unless otherwise stated below.

For surface coverages in the multilayer regime, multi-dimensional nucleation and crystal growth is expected at the disorder-to-order transition. In order to model the disorder-to-order transition in biphenyl as a nucleation-crystallization process, the Johnson-Mehl-Avrami-Kolmogorov, JMAK, or simply, Avrami model was used.<sup>11-13</sup> In the simplest form, the Avrami equation describes a sigmoidal curve and is given by:<sup>11-13</sup>

$$I(t) = 1 - e^{-kt^n} \quad (1)$$

where  $I(t)$  is the time dependent fluorescence intensity at the disorder-to-order transition that is converted to fraction of the disordered state at the transition,  $k$  is related to the rate with which nucleation and growth by crystallization occurs and is in part, a function of the density of nucleation sites,  $t$  is time in s and  $n$  is the dimensionless Avrami exponent that yields the dimensionality of the nucleation-crystallization process.<sup>11-13</sup> The  $n$  is also a function of whether nucleation is instantaneous ( $n_N = 0$ ) or sporadic ( $n_N = 1$ ), where  $n = n_G + n_N$ , and  $n_G$  is the dimensionality of growth.<sup>11-13</sup> Growth may be spheres for  $n_G = 3$ , plates for  $n_G = 2$  and needles for  $n_G = 1$ .<sup>11-13</sup> The unit for  $k$  is the inverse of time raised to the  $n^{\text{th}}$  power. This expression was made to fit the wavelength-resolved TPD data at the disorder-to-order transition using algorithms provided by SciPy (an open-source Python library) and automated with Python (an open-source programming language, Python Software Foundation) in which the parameters were controlled by user interface.

The Python curve fitting program was tested according to the procedure given in the Supporting Information with simulated sigmoidal functions in which the  $n$  and  $k$  values were varied. These values were then returned by the curve fitting program with good

reproducibility. Additionally, for biphenyl and naphthalene multilayers, spreadsheet plots of equation 2 in the Supporting Information section were used to determine  $n$  and  $k$  values from the trend-line equation. These were consistent with the results obtained by the curve fitting program. Having validated the program, it was then used to determine the  $n$  and  $k$  values of multiple runs of each system. Results were within  $\pm 20$  and  $\pm 50$  % for  $n$  and  $k$  values, respectively and these errors were then used in this report.

## Results and Discussion

### Biphenyl Multilayer

Shown in Figure 1 is a representative fluorescence wavelength-resolved TPD of a biphenyl multilayer (neat, single adsorbate). The arrangement of biphenyl molecules in the vapor deposited adlayer is known to be amorphous, glassy and disordered with a  $\lambda_{\text{max}}$  at 316 nm.<sup>1-7</sup> At 160 K during the TPD, the adlayer underwent a transition from disorder to a more ordered arrangement that is characterized by the  $\lambda_{\text{max}}$  red-shift to 338 nm. In this ordered arrangement, exciton resonant energy transfer pathways compete with the radiative relaxation and quench the fluorescence to  $\sim 15$  % of the initial intensity. The peak desorption temperature,  $T_p$ , of neat biphenyl at low coverages was 229 K. First-order desorption was assumed and the activation energy for desorption,  $E_a$ , was calculated to be  $60 \text{ kJ mol}^{-1}$ .<sup>8-10</sup>

The output from the curve fitting program is shown in Figure 2. Here,  $n = 4.2 \pm 0.8$  and  $k = 0.28 \pm 0.13$ . Again,  $k$  is a function of nucleation and crystal growth rate.<sup>11-13</sup> It is related to the geometry of the nuclei, which in this case would be presumed to be spherical.<sup>11-13</sup> The  $n_G$  is a function of the dimensionality of growth, 3, and nucleation is sporadic with  $n_N = 1$ .<sup>11-13</sup>

### Methanol/biphenyl bilayer

Shown in Figure 3 is the wavelength-resolved TPD of a bilayer composed of methanol and biphenyl, in which the methanol functions as an impurity that impedes biphenyl's ordering process. The desorption temperature of methanol was 139 K and

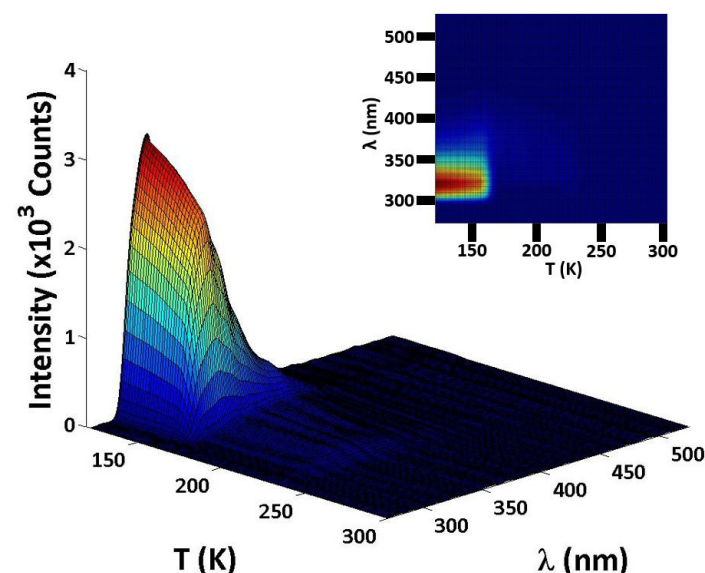


**Figure 1.** Wavelength-resolved TPD of biphenyl with a  $\lambda_{\text{max}}$  at 316 nm. The disorder-to-order transition occurred at about 160 K and  $\lambda_{\text{max}}$  red-shifted to 338 nm, barely visible.  $\Theta_{\text{biphenyl}} \sim 154 \text{ ML}$ . Inset: top view.

the activation energy for desorption was calculated to be  $35.6 \text{ kJ mol}^{-1}$ .<sup>8-10</sup> The effect on the disorder-to-order transition was quite dramatic, in that the curve fitting program yielded  $n$  of  $1.8 \pm 0.4$  and  $k = 0.058 \pm 0.030$  and is shown in Figure 4. Percolation of methanol was postulated to cause biphenyl molecules to become

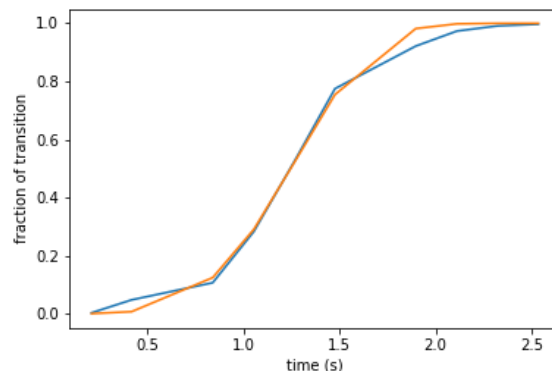


**Figure 2.** Output from the curve fitting program for biphenyl multilayer,  $\Theta_{\text{biphenyl}} \sim 100 \text{ ML}$ . Wavelength = 316 nm, Temperature range = 159-165 K. Avrami  $n = 4.2 \pm 0.8$  and  $k = 0.28 \pm 0.13$ . Data in blue and best fit with the  $n$  and  $k$  values is in red.

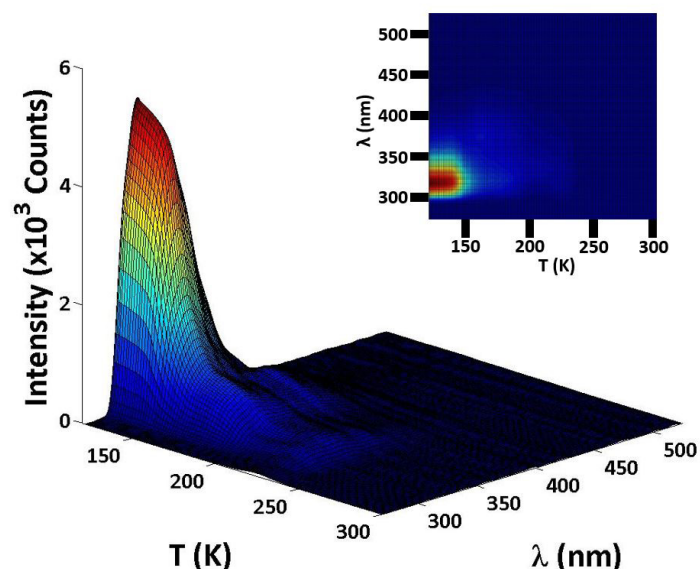


**Figure 3.** Wavelength-resolved TPD of methanol/biphenyl bilayer with biphenyl as the upper layer.  $\Theta_{\text{methanol}} \sim 26 \text{ ML}$  and  $\Theta_{\text{biphenyl}} \sim 96 \text{ ML}$ . Inset: top view.

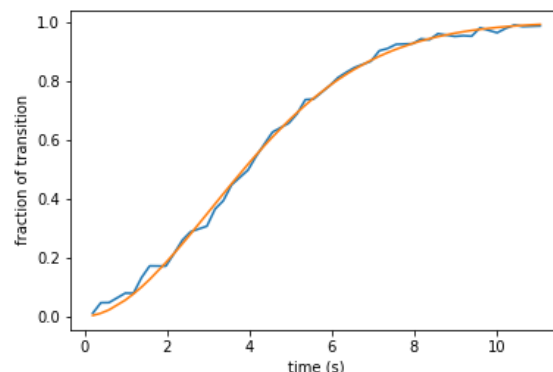


**Figure 4.** Output from the curve fitting program for methanol/biphenyl bilayer.  $\Theta_{\text{methanol}} \sim 67 \text{ ML}$  and  $\Theta_{\text{biphenyl}} \sim 97 \text{ ML}$ . Wavelength = 316 nm, Temperature range = 159-165 K. Avrami  $n$  of  $1.8 \pm 0.4$  and  $k = 0.058 \pm 0.030$ . Data in blue and best fit with the  $n$  and  $k$  values is in red.

less mobile, thereby disrupt biphenyl's cooperative domains that were required for ordering.<sup>14,15</sup> Nucleation domains most likely became smaller and more isolated by methanol percolation.<sup>14,15</sup>

### Naphthalene multilayer

The wavelength-resolved TPD of naphthalene is shown in Figure 5. The adlayer that formed when naphthalene was vapor deposited on  $\text{Al}_2\text{O}_3$  was amorphous and optical pumping exhibited excimer fluorescence.<sup>1-7</sup> During the TPD, the adsorbate transitioned from the amorphous morphology to a more ordered state that occurred 200 K, just prior to desorption. The desorption temperature was 212 K and the calculated energy of desorption was  $54.8 \text{ kJ mol}^{-1}$ .<sup>8-10</sup>

Shown in Figure 6 is the output from the curve fitting program that resulted in  $n = 2.3 \pm 0.5$  and  $k = 0.021 \pm 0.011$ . The  $n$  is a function of the dimensionality of growth and whether nucleation is instantaneous ( $n_N = 0$ ) or sporadic ( $n_N = 1$ ),<sup>11-13</sup> and is consistent with  $n$  value of 2 obtained for phenanthrene by previous researchers.<sup>16</sup> Since naphthalene grows by packing directed by van der Waals interaction direct the edge-to- $\pi$  type packing of naphthalene that is thought to result in 2-dimensional plates or  $n_G = 2$ .<sup>15</sup> Since such bonding is non-directional, surface diffusion is important.<sup>15</sup> This would mean that  $n_N = 1$  or sporadic nucleation would be expected.<sup>11-13</sup>

### Methanol/naphthalene

Shown in Figure 7 is the wavelength-resolved TPD of a bilayer of methanol as the underlayer and biphenyl as the overlayer. The curve fitting result indicated that  $n = 1.1 \pm 0.2$  and  $k = 0.25 \pm 0.13$ . If, the growth was one-dimensional due to the percolation of methanol that impedes the mobility of naphthalene molecules,  $n_N$  most likely must be 0, or instantaneous nucleation.<sup>11-13</sup>

### Conclusion

In summary, curve fitting programs appear to be useful in classifying and describing the type of nucleation-crystallization ki-

netics that occur during the disorder-to-order transition in biphenyl and naphthalene that were vapor deposited on  $\text{Al}_2\text{O}_3$ . Nucleation and growth for glassy biphenyl was spherical with sporadic nucleation. For naphthalene the growth was also sporadic but was more plate-like. The introduction of an impurity, methanol in this study,

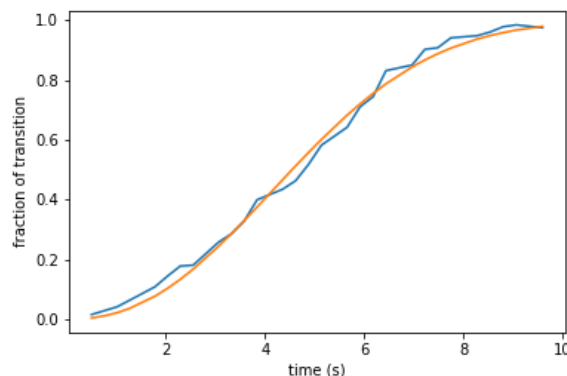


**Figure 6.** Output from the curve fitting program for naphthalene multilayer.  $\Theta_{\text{naphthalene}} \sim 92 \text{ ML}$ . Wavelength = 396 nm, Temperature range = 200-220 K. Avrami  $n = 4.2 \pm 0.8$  and  $k = 0.28 \pm 0.13$ . Data in blue and best fit with the  $n$  and  $k$  values.

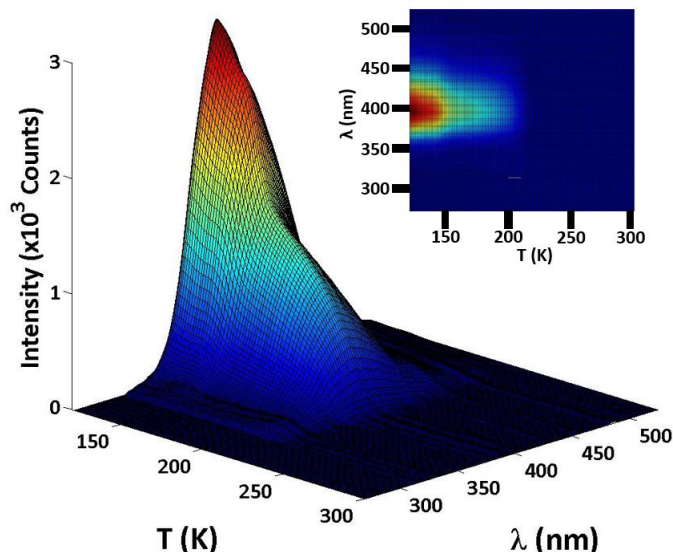


**Figure 7.** Wavelength-resolved TPD of methanol/naphthalene bilayer with naphthalene on top.  $\lambda_{\text{max}}$  at 396 nm. The disorder-to-order transition occurred at about 200 K.  $\Theta_{\text{methanol}} \sim 29 \text{ ML}$  and  $\Theta_{\text{naphthalene}} \sim 17 \text{ ML}$ . Inset: top view.

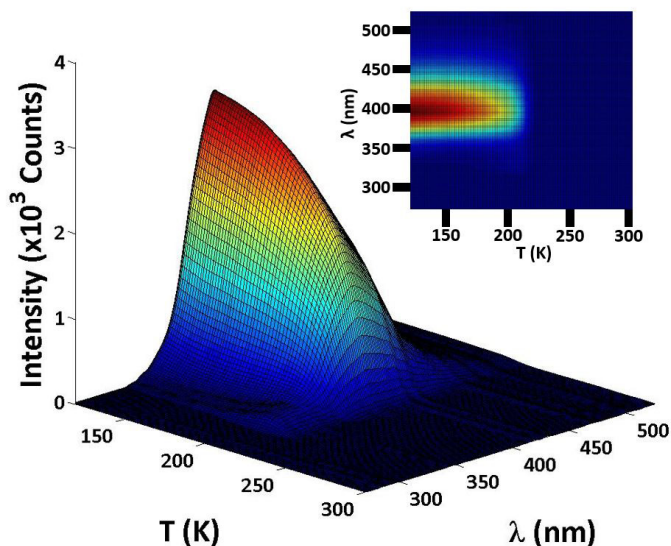


**Figure 5.** Wavelength-resolved TPD of naphthalene multilayer with a  $\lambda_{\text{max}}$  at 396 nm. The disorder-to-order transition occurred at about 200 K, as indicated by the precipitous decrease in intensity and concomitant emergent blue-shifted trap fluorescence that is barely visible.  $\Theta_{\text{biphenyl}} \sim 92 \text{ ML}$ . Inset: top view.

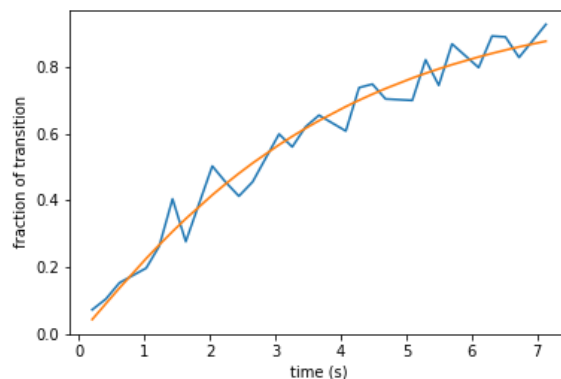


**Figure 8.** Output from the curve fitting program for methanol/naphthalene bilayer.  $\Theta_{\text{methanol}} \sim 29 \text{ ML}$  and  $\Theta_{\text{naphthalene}} \sim 17 \text{ ML}$ . Wavelength = 396 nm, Temperature range = 150-165 K. Avrami  $n = 1.1 \pm 0.2$  and  $k = 0.25 \pm 0.13$ . Data in blue and best fit with the  $n$  and  $k$  values is in red.



caused the dimensionality to decrease dramatically, presumably due to the domains that were more isolated as methanol percolated through the chromophoric adlayers.

## Acknowledgment

The authors would like to thank the John Stauffer Charitable Trust for funding the student stipends for summer research. This work was supported by the donors of ACS Petroleum Research Fund under Undergraduate Research #68385-UR5 and -S24.

## References

1. Karli R. Holman, Xianzhang Geng, K.A. Martin and A.M. Nishimura, *J. Lumin.*, **2017**, 181, 19-24.
2. B.D. Fonda, M.K. Condi, Z.E. Moreau, Z.I. Shih, B. Dionisio, A. Fitts, L. Foltz, K. Nili and A.M. Nishimura. *J. Phys. Chem. C.*, **2019**, 123, 26185-26190.
3. M.K. Condie, B.D. Fonda, Z.E. Moreau and A.M. Nishimura, *Thin Solid Films*, **2020**, 697, 137823-137828.
4. Nicole M. Bond and A.M. Nishimura, *JUCR*, **2022**, 21, 84-92.
5. I.Z. Song, S.T. Watanabe and A.M. Nishimura, *JUCR*, **2023**, 22 1-8.
6. J.M. Rosenfeld, R.M. Toepfer, A.O. Lopez, J.C. Nieman, I. Felix, J. Zerwas and A.M. Nishimura, *JUCR*, **2024**, 23, 25-30.
7. B.X. Moses, C.D. Tobey, A.O. Lopez and A.M. Nishimura, *JUCR*, **2025**, 24, 66-72.
8. P.A. Redhead. *Vacuum*, **1962**, 12, 203-211.
9. F.M. Lord and J.S. Kittelberger. *Surf. Sci.*, **1974**, 43, 173-182.
10. D.A. King. *Surf. Sci.*, **1975**, 47, 384-402.
11. M. Avrami, *J. Chem. Phys.*, **1939**, 7, 1103-1112.
12. M. Avrami, *J. Chem. Phys.*, **1940**, 8, 212-224.
13. K. Shirzad and C. Viney, *J. Roy. Soc. Interface.* **2023**, 20. <https://doi.org/10.1098/rsif.2023.0242>.
14. T. Suthan, N.P. Rajesh, P.V. Dhanaraj and C.K. Mohadevan, *Spectrochim. Acta A: Molec. Biomolec Spectroscopy.* **2010**, 75, 1. <https://doi.org/10.1016/j.saa.2009.09.041>.
15. P. Yu, Y. Zhen, H. Dong and W. Hu, *Cellpress Reviews Chem* **2019**, 5, 2814-2853.
16. N.J. Tro, A.M. Nishimura, D.R. Haynes and S.M. George, *Surface Science Lett.* **1989**, 207, L961-L970.

## Supporting Information

### Validating the Python Curve Fitting Program

The Avrami equation describes a sigmoid function given by equation 1 in the Experimental section above, where  $k$  and  $n$  are the Avrami constants that describe the nucleation-crystallization kinetics.<sup>11-13</sup> Here, the  $k$  value is a function of nucleation and growth rate and it is related to the geometry of the nuclei.<sup>11-13</sup> As mentioned previously,  $n$  is a function of the dimensionality of growth, and whether nucleation is instantaneous ( $n_N = 0$ ) or sporadic ( $n_N = 1$ ), where  $n = n_G + n_N$ .<sup>11-13</sup> If the nucleation rate vary with time,  $n_N$  will be  $> 1$ .<sup>12-14</sup>

Growth mechanism for disorder-to-order transitions is thought to be interface-controlled, and grow linearly in time and is classified as sporadic.<sup>11-13</sup> In such cases, spherical growth result in  $n = 4$ . If  $n = 3$ , plate-like growth and needle-like growth will result in  $n = 3$ , and  $n = 2$ , respectively.<sup>11-13</sup>

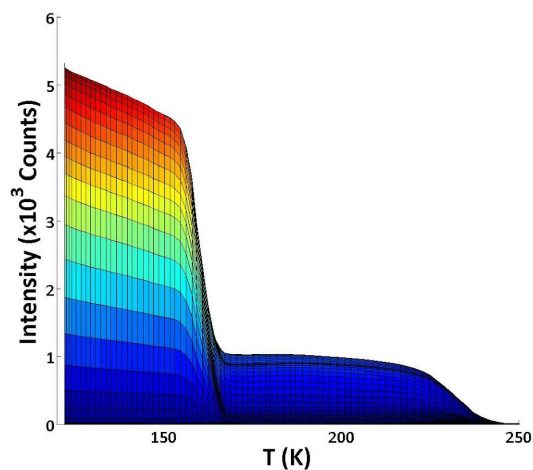


**Figure S1.** Wavelength-resolved TPD of biphenyl with a  $\lambda_{\text{max}}$  at 316 nm. The disorder-to-order transition occurred at about 160 K and  $\lambda_{\text{max}}$  red-shifted to 338 nm.

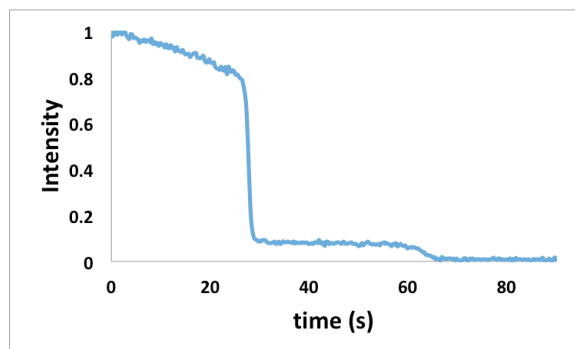


**Figure S2.** Biphenyl fluorescence intensity versus time at 316 nm. The disorder-to-order transition occurred at 22 - 31 s.

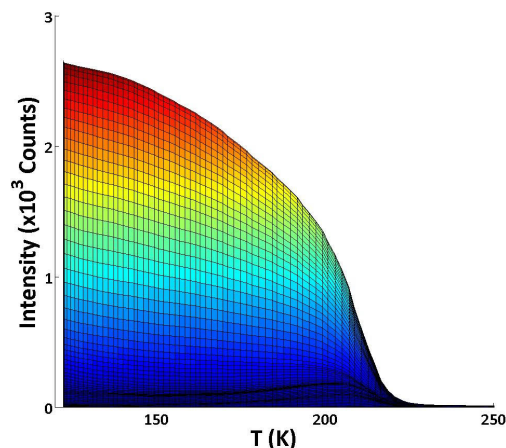


**Figure S3.** Wavelength-resolved TPD of naphthalene with a  $\lambda_{\text{max}}$  at 396 nm. The disorder-to-order transition occurred at about 200 K.

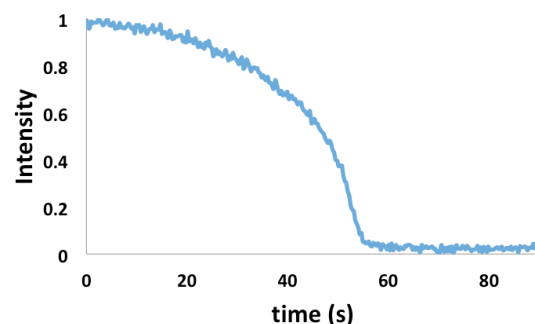


**Figure S4.** Naphthalene fluorescence intensity versus time at 396 nm. The disorder-to-order transition occurred at 42 - 52 s.

In order to thoroughly test the Python curve fitting routine, simulated Avrami equation with variable  $n$  and  $k$  values were created. Repeated runs yielded the  $n$  and  $k$  values within  $\pm 20$  and 50 %, respectively, and this error was used throughout this study.

By visual inspection, the range in time were adjusted so that the curve fitted well. This also allowed a more accurate temperature range during which the disorder-to-order transition occurred. In addition, the precision of the ramp rate through the TPD gave a good time conversion for Python to fit the data to the Avrami equation. It should be noted that the data along the x-axis were converted to time during the TPD because the ramp rate was fixed at  $2.0 \text{ K s}^{-1}$ .

If the natural logarithm of the Avrami equation (1) is taken twice, a linear equation is derived:

$$\ln[-\ln\{1-f(t)\}] = n \ln(t) + \ln(k) \quad (2)$$

Linear fits of the slices of intensities versus temperature yielded the  $n$  and  $k$  values. Equation 2 was used to manually double-check the Python curve fitted  $n$  and  $k$  values for both biphenyl (Shown in Figures S1 and S2) and naphthalene multilayer data that are shown in Figures S3 and S4. Spreadsheet software was used for this manual checking. This procedure gave confidence that the Python routine was yielding reasonable  $n$  and  $k$  values.

It should be noted that the  $n$  value should not exceed 4; otherwise, assumptions of the Avrami model do not hold.<sup>11-13</sup> Particular care had to be taken when analyzing the biphenyl multilayer data. The range in sigmoid that describe the fraction of the transition was narrowed to between 0.1 and 0.9<sup>11-13</sup> when necessary so as to not go against this restriction on the  $n$  value.